

Observation of an Unstable $l = 1$ Diocotron Mode on a Hollow Electron Column

C. F. Driscoll

University of California at San Diego, La Jolla, California 92093

(Received 11 September 1989)

Stable and unstable diocotron modes varying as $e^{i\theta}$, with $l=1$, are measured on a magnetized, partially hollow electron column. The unstable mode is observed to grow exponentially over several decades, in contradiction to present 2D fluid theory. This $l=1$ instability can dominate the evolution well into the nonlinear regime, resulting in cross-field transport to a stable, monotonically decreasing density profile. To the extent this process is described by 2D $\mathbf{E} \times \mathbf{B}$ drifts, it is isomorphic to the Kelvin-Helmholtz shear-flow instability of inviscid fluids.

PACS numbers: 52.25.Wz, 47.20.Ft, 52.35.Fp

Diocotron waves and instabilities are observed in many nonneutral, magnetized beam or plasma devices. These electrostatic waves are charge perturbations which execute $\mathbf{E} \times \mathbf{B}$ drifts in the unneutralized self-electric-field; in cylindrical geometry the spatial variations can be written $\delta n(r) \exp[i(l\theta + ik_z z)]$, with k_z often zero. The diocotron instability arises due to shears in the rotational drift velocity; it was first utilized in the operation of magnetrons,¹ but is often an unwanted degradation in the propagation of hollow or ribbon beams.²⁻⁶ More recently, linear and nonlinear diocotron waves have been studied in detail on stable⁷⁻¹¹ and unstable charge-density profiles.^{12,13}

To the extent the charge column can be considered a two-dimensional drift system (i.e., strongly magnetized, $k_z=0$, and no significant axial dynamics), it evolves as a 2D inviscid fluid. Specifically, the 2D drift-Poisson equations are isomorphic to the 2D Euler equations for a uniform density fluid.⁵ Furthermore, the charge density (which we measure) is proportional to the vorticity of the flow. The stable and unstable diocotron modes are thus examples of surface waves and the Kelvin-Helmholtz instability on an extended vortex.

Stability analyses of these systems often consider "step" profiles in charge density (or vorticity).^{5,11,14} Then, one mode arises from each density step, and complex-conjugate modes appear as a prediction of exponential instability. Alternately, one can numerically compute eigenvalues for smooth density profiles. For azimuthal mode number $l=1$, linear theory predicts that there are no exponentially unstable modes no matter what the density profile is,^{5,11} unless there is a central conductor.¹² More recently, an initial-value theory suggested that there may be an algebraically growing $l=1$ instability for hollow profiles.¹⁵ For $l \geq 2$, experiments have observed stable and unstable modes with frequencies and growth rates in rough agreement with computed eigenvalues.¹³

Here, we present detailed experimental measurements of simultaneously coexisting stable and unstable $l=1$, $k_z=0$ diocotron waves on partially hollow electron columns. The two waves are not a complex-conjugate pair.

Characteristics of the stable wave agree well with theory. However, the unstable wave is observed to grow exponentially over several decades, in apparent contradiction to theory. This unstable wave can dominate the dynamics well into the nonlinear regime, where substantial cross-field transport occurs. In essence, an $l=1$ instability turns the plasma "inside out," resulting in a stable density profile.

The pure electron plasmas are contained in a grounded conducting cylinder,¹⁶ as shown in Fig. 1. A uniform axial magnetic field ($B_z=375$ G) provides radial confinement, and negative voltages (-50 V) applied to end cylinders *A* and *C* provide axial confinement. The apparatus is operated in an inject-manipulate-dump cycle. For injection, cylinder *A* is briefly grounded, allowing electrons to enter from the negatively biased (-23 V at center) tungsten-filament source. The trapped electrons can be contained for hundreds of seconds,¹⁶ and can be manipulated in a variety of ways.

For this experiment, we apply a small $l=1$ "seed" asymmetry to a quiescent, azimuthally symmetric column, then make the density profile hollow, and then measure the resulting instability. The seed asymmetry is the result of transmitting a (stable) $l=1$, $k_z=0$ diocotron wave of controlled amplitude and phase, using iso-

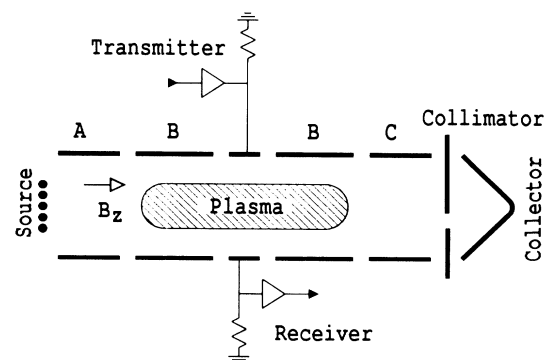


FIG. 1. Schematic diagram of the cylindrical containment apparatus.

lated 60° wall sectors.^{8,10} The density profile is then made partially hollow by decreasing the containment voltage on cylinder A (to -18 V for about $1 \mu\text{s}$), thereby ejecting some electrons near $r=0$. (The source is biased positive during ejection.)

At any time t after ejection, we can obtain the z -averaged plasma density by grounding cylinder C , thereby dumping the plasma. We measure the charge Q which flows along B_z through a collimator hole of area $A_h = \pi(1.6 \text{ mm})^2$, giving the density¹⁶

$$n(r, \theta, t) \equiv \int dz \bar{n}/L_p = Q/(-eA_h L_p).$$

Only one density measurement is obtained on each machine cycle, but shot-to-shot variations are less than 0.1%. We obtain the temporal dependence by varying the evolution time t between ejection and dump, and the spatial dependence by varying the position r of the radially scanning collimator hole, and the phase θ of the seed asymmetry at the time of ejection.

The plasmas considered here have local densities $\bar{n} \approx 5 \times 10^6 \text{ cm}^{-3}$ out to a radius $R_p \approx 2 \text{ cm}$ over an axial length $L_p \approx 30 \text{ cm}$, and are contained in a cylinder of radius $R_w = 3.81 \text{ cm}$. The unneutralized space charge gives a radial electric field $E_r \lesssim -7 \text{ V/cm}$, resulting in an $\mathbf{E} \times \mathbf{B}$ rotation frequency of $f_E \lesssim 140 \text{ kHz}$. The electrons have a characteristic thermal energy $kT \approx 1.2 \text{ eV}$; this gives a cyclotron radius $r_c \approx 60 \mu\text{m}$, and an axial "bounce" rate $f_b \approx v_{\parallel}/2L_p \approx 800 \text{ kHz}$, so $f_b \gg f_E$.

A typical hollow-plasma evolution is shown in Fig. 2. The initial seed asymmetry, shown at $t = 10 \mu\text{s}$, has two components: The center of mass (c.m.) of the plasma column is displaced off the cylindrical axis by 0.85 mm , and the central density minimum is not centered in the

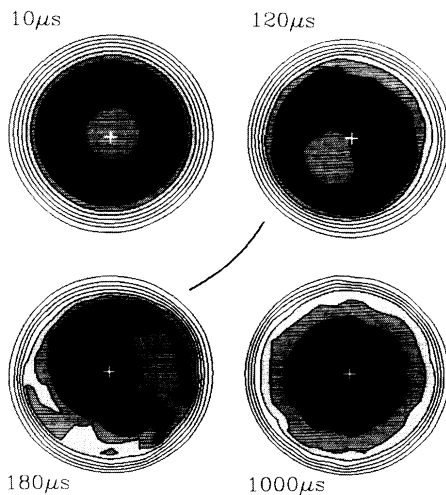


FIG. 2. Contour plots of the z -averaged density $n(r, \theta)$ at four times during the $l=1$ instability. The contours are in increments of $0.6 \times 10^6 \text{ cm}^{-3}$, and the highest four levels are shaded from gray to black.

plasma. We observe that the c.m. orbits about the axis at $f_s = 38.9 \text{ kHz}$, with constant orbit size (this is the stable mode). Similarly, the low-density region orbits about the c.m. at $f_u = 143.4 \text{ kHz}$, but it spirals outward with time (this is the unstable mode). The high-density ring collapses in θ into a high-density region, as shown at $t = 120 \mu\text{s}$. Eventually, the high-density region moves to the center and the low-density region spreads out in θ at an appropriate radius, as shown at $t = 180 \mu\text{s}$. Most θ variations (with respect to the c.m.) have been eliminated by $t = 1000 \mu\text{s}$.

The initial stages of this evolution can be analyzed from the perspective of linear modes, and our data for $n(r, \theta, t)$ characterize the $k_z = 0$ modes rather completely. We consider the $l=1$ component of the data, given by

$$\delta n(r, t) \equiv \int_0^{2\pi} d\theta n(r, \theta, t) e^{i\theta}. \quad (1)$$

We observe that two frequency components are present in these data, and that these frequencies do not vary with radius. Thus, the $l=1$ data component can be computationally fitted by a sum of two modes, as

$$\delta n(r, t) = \sum_q \delta n_q(r) e^{i2\pi f_q t} e^{\gamma_q t}, \quad (2)$$

with $q = s, u$. This least-squares fit determines the mode frequencies f_q , growth rates γ_q , and radial eigenfunctions $\delta n_q(r)$. Of course, the term "eigenfunction" here refers to the radial dependence of the measured oscillations, rather than to the theory of linear operators.

Figure 3 shows the amplitudes and phases of the radial eigenfunctions δn_s and δn_u (normalized to unity), obtained from an evolution similar to that of Fig. 2. Also

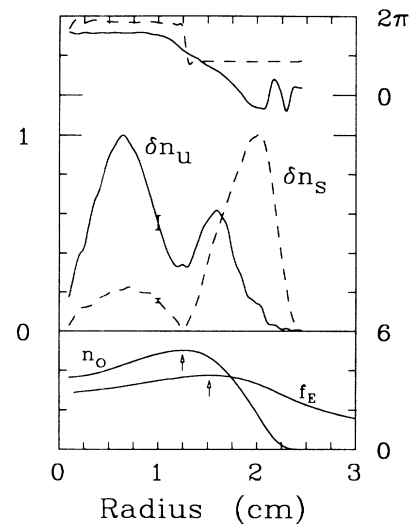


FIG. 3. Amplitudes and phases of the measured stable and unstable eigenfunctions $\delta n_s(r)$ and $\delta n_u(r)$. Also shown are the initial hollow density profile $n_0(r)$ (units 10^6 cm^{-3}) and the initial $\mathbf{E} \times \mathbf{B}$ drift rotation $f_E(r)$ (units 40 kHz).

shown for reference are the density $n_0(r)$ and the $\mathbf{E} \times \mathbf{B}$ rotation frequency $f_E(r)$. This fit used data at fifty radii and eleven times. The standard errors for the eigenfunctions, obtained by presuming the residual arises from random noise, are shown as error bars at $r=1$. Fitting with three modes would not substantially decrease the residual.

The eigenfunction δn_s represents the stable orbit of the entire hollow plasma column about the cylindrical axis: The amplitude and phase are well approximated by $\delta n_s(r) \propto \partial n_0 / \partial r$, as predicted by linear theory.⁵ This mode appears to have the same general characteristics for either monotonic or hollow density profiles, with a frequency $\approx f_E(R_w)$.

The unstable mode arises only for density profiles which are at least partially hollow. The eigenfunction δn_u is approximately proportional to $\partial n_0 / \partial r$ inside the radius r_n defined by the maximum of $n_0(r)$; for $r \gtrsim r_n$, there is another contribution with varying phase which appears to be unrelated to $\partial n_0 / \partial r$. The unstable-mode frequency f_u equals the maximum of $f_E(r)$, to within the experimental accuracy of $\pm 3\%$ in determining $f_E(r)$. Interestingly, this mode is largely self-shielding: The calculated electric field arising from the mode is essentially zero outside the plasma.

We can obtain the actual time evolution of the mode amplitudes, $A_q(t)$, by "projecting" the original data onto these two eigenfunctions, as

$$\delta n(r,t) = \sum_q A_q(t) \delta n_q(r). \quad (3)$$

In this fit, there is no presumption of exponential growth, as there is in Eq. (2). The residual is small until late in the evolution, when nonlinearities or other unstable

modes become significant.

Figure 4 shows the magnitude of the mode amplitudes versus time for four initial seed perturbations in 10-dB steps. In all cases, $A_u(t)$ exhibits what appears to be exponential growth, followed by nonlinear saturation, whereas $A_s(t)$ is essentially constant. For the smallest seed, this exponential growth covers more than two decades. The straight lines represent exponential growth with $\gamma_u = 23.3$ kHz, and are separated by 10 dB. The eigenfunctions of Fig. 3 were obtained from the data represented by the cluster of crossed circles from 40 to 50 μs . Figure 2 was obtained from the evolution represented by the diamonds.

The initial instability appears to be a linear process, as evidenced by the parallel growth curves in Fig. 4. Further, the mode saturates at a reasonable level: The saturation level of $A_u \sim 0.3$ represents (due to complex conjugates) a sinusoidal amplitude of 0.6, or a peak-to-peak amplitude of 1.2. This results from the difference between the central minimum (3.6) and the maximum (5.0) value of $n_0(r)$.

The instability seems to be mainly a 2D drift effect. We observe conservation (to reasonable experimental accuracy) of the total number of electrons, the total angular momentum, the 2D electrostatic energy, and the perpendicular temperature.¹⁶ The most striking difference from simple 2D drift dynamics is the variation in the measured histogram of $A(n)$, defined as the r - θ area A which has a given density n . In incompressible flow, $A(n)$ does not vary with time. The measured $A(n)$ varies substantially, often including a 5% increase in the maximal density. Consequently, moments of $A(n)$ such as the enstrophy vary substantially also. We do not at present know how much of this is due to finite-length effects, due to coarse graining over the area of the collimator hole, or due to nontrivial z dynamics.

The appearance of exponential growth for the unstable mode is not an artifact of the fitting process of Eqs. (2) and (3): The exponential growth can be seen directly from $\delta n(r,t)$ with no fitting. The small open circles of Fig. 4 show $\delta n(r_m,t)$, which is the maximum magnitude of $\delta n(r,t)$ (restricted to $r_m < r_n$, so as to emphasize the unstable mode), for the evolution where A_u is shown by solid circles. The small circles are initially somewhat above the solid circles, because the stable and unstable modes happen to add in phase. For $t > 80 \mu s$, $A_u > A_s$, so the superposition matters less, and the $\delta n(r_m,t)$ data agree well with the fit.

We have eliminated a number of effects as possible causes of the observed exponential instability. First, we have established that the instability is not a coupling to the stable $l=1$, $k_z=0$ diocotron mode. As seen from Fig. 3, $A_s \approx 9A_u$ at $t=0$. However, even when we feedback damp the stable mode by 20 dB within $\frac{1}{2}$ period after $t=0$, the same exponential instability is observed. Similarly, we have established that the instability is not a

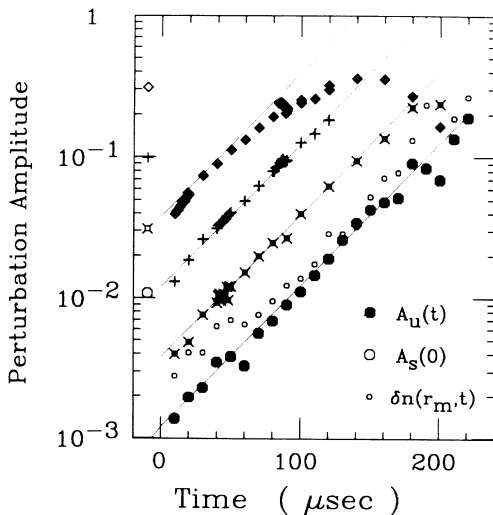


FIG. 4. Amplitude of the unstable mode $A_u(t)$ (solid symbols) for four different initial seed amplitudes (units 10^6 cm^{-3}). Open symbols placed at $t < 0$ show the initial amplitude A_s of the stable mode.

coupling to the $l=0$, $k_z \neq 0$ plasma modes which tend to be excited by the process of ejection at $t=0$: Damping these modes by resistive dissipation in the axial direction makes no difference in the instability evolution. Next, we have established that the instability is unaffected by small angular misalignment ($\approx 10^{-3}$ rad) between the magnetic and cylindrical (electrostatic) axes; this "tilt" misalignment tends to make $l=1$, $k_z \neq 0$ oscillations appear, but does not affect the instability evolution. Similarly, the instability evolution is independent of the (azimuthal) resistances⁸ used on the wall sectors for receiving and transmitting waves. Finally, we note that the instability occurs over a broad range of plasma lengths L_p , although very short plasmas may show no instability for any l mode.¹⁶

In summary, we have observed coexisting stable and unstable $l=1$ diocotron modes on partially hollow electron columns. The unstable mode appears to grow exponentially over a range of several decades, in contradiction to present 2D fluid theory.

The author would like to acknowledge useful discussions with K.S. Fine, R. W. Gould, J. H. Malmberg, T. M. O'Neil, M. N. Rosenbluth, and R. A. Smith. This work was supported by ONR (N00014-82-K-0621), NSF (PHY87-06358), and DOE (DE-FG03-85ER53199).

¹*Crossed-Field Microwave Devices*, edited by G. Okress

(Academic, New York, 1961).

²H. F. Webster, *J. Appl. Phys.* **26**, 1386 (1955).

³C. A. Kapetanokos *et al.*, *Phys. Rev. Lett.* **30**, 1303 (1973).

⁴K. M. Case, *Phys. Fluids* **3**, 143 (1960).

⁵R. H. Levy, *Phys. Fluids* **8**, 1288 (1965); **11**, 920 (1968).

⁶R. J. Briggs, J. D. Daugherty, and R. H. Levy, *Phys. Fluids* **13**, 421 (1970).

⁷J. S. deGrassie and J. H. Malmberg, *Phys. Fluids* **23**, 63 (1980).

⁸W. D. White, J. H. Malmberg, and C. F. Driscoll, *Phys. Rev. Lett.* **49**, 1822 (1982).

⁹S. A. Prasad and T. M. O'Neil, *Phys. Fluids* **26**, 665 (1983).

¹⁰K. S. Fine, C. F. Driscoll, and J. H. Malmberg, *Phys. Rev. Lett.* **63**, 2232 (1989).

¹¹R. C. Davidson, *Theory of Nonneutral Plasmas* (Benjamin, New York, 1974), Sec. 2.10.

¹²G. Rosenthal, G. Dimonte, and A. Y. Wong, *Phys. Fluids* **30**, 3257 (1987).

¹³C. F. Driscoll *et al.*, in Proceedings of the Twelfth International Conference on Plasma Physics and Controlled Nuclear Fusion Research, Nice, France, 1988 (IAEA, Vienna, to be published).

¹⁴Lord Rayleigh, *Scientific Papers of Lord Rayleigh* (Dover, New York, 1964), Vol. I, p. 474.

¹⁵R. A. Smith *et al.*, *Bull. Am. Phys. Soc.* **33**, 1898 (1988); R. A. Smith and M. N. Rosenbluth, following Letter, *Phys. Rev. Lett.* **64**, 649 (1990).

¹⁶C. F. Driscoll, J. H. Malmberg, and K. S. Fine, *Phys. Rev. Lett.* **60**, 1290 (1988).

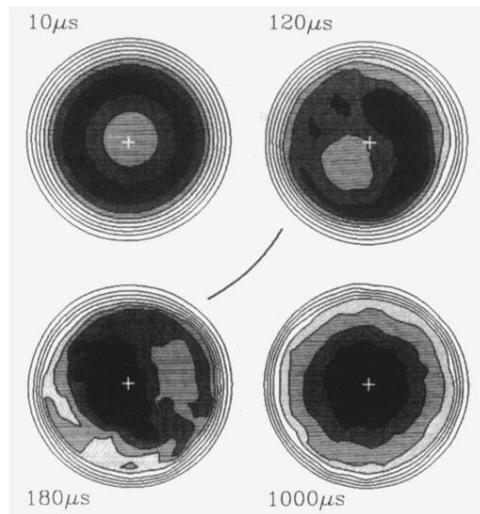


FIG. 2. Contour plots of the z -averaged density $n(r, \theta)$ at four times during the $l=1$ instability. The contours are in increments of $0.6 \times 10^6 \text{ cm}^{-3}$, and the highest four levels are shaded from gray to black.